

See discussions, stats, and author profiles for this publication at: <https://www.researchgate.net/publication/224401379>

# Modeling and motion planning of the infant-size humanoid robot THBIP-II

Conference Paper · January 2008

DOI: 10.1109/ICHR.2007.4813929 · Source: IEEE Xplore

CITATIONS

4

READS

38

3 authors, including:



Zeyang Xia

Chinese Academy of Sciences

59 PUBLICATIONS 174 CITATIONS

[SEE PROFILE](#)



Ken Chen

Albert Einstein College of Medicine

110 PUBLICATIONS 742 CITATIONS

[SEE PROFILE](#)

Some of the authors of this publication are also working on these related projects:



Linking Robotics to Orthodontics [View project](#)

All content following this page was uploaded by Zeyang Xia on 28 May 2014.

The user has requested enhancement of the downloaded file.

# Modeling and Motion Planning of the Infant-size Humanoid Robot THBIP-II

Zeyang Xia\*, Ken Chen\*, Yeming He<sup>#</sup>

\*Robotics and Automation Laboratory, Department of Precision Instruments and Mechanology,  
Tsinghua University, Beijing, 100084, China

<sup>#</sup>Ningbo Mecai Car Circler Co., Ltd, Zhejiang, 315191, China  
zeyang.xia@ieee.org

**Abstract** — The infant-size humanoid robot THBIP-II, Tsinghua University biped robot II, is the second generation prototype of Tsinghua biped robots. THBIP-II is 75 cm tall, weighs 18 Kg, and has 24 degrees of freedom (DOF). This paper addresses the design, mechanical modeling, gait planning method, and global footstep planning method of the robot. First the humanoid mechatronics system and its kinematics and dynamics modeling are prescribed. Second, the gait planning algorithm developed for human-like walking is presented. Third, a footstep planning method for global navigation is addressed. Finally, the walking experiments are given to verify the validity of the above aspects.

## I. INTRODUCTION

Since the first biped robot, Wabot-1, was developed in 1973 [1], there has been rapid progress from simple biped robots to the advanced humanoid robots being built today. The original motivation for developing humanoid robots was to build robots that resemble human behaviors regarding locomotion, manipulation and intelligence. This objective remains to make robots that coexist with, collaborate with, and serve humans, even performing tasks that are dangerous or not feasible for humans. Achieving these functionalities requires innovation in several broad research fields, and many researchers around the world focus on these topics. Some researches concentrate on the locomotion theories [2]-[6], some on the system integration and intelligence [7]-[9], while others focus on fundamental scientific fields, such as new actuation methods [10].

In recent years several successful humanoid robots have been unveiled, specifically the Honda and Sony humanoid robots which have achieved complex locomotion patterns and a high level of intelligence exhibited by their audio and video communication with the humans [8][11]. However, general research on humanoid robotics is still in its elementary period and there are still basic issues to be studied. System design, gait planning and walking control are still pivotal technologies and have been a bottleneck for advancement of the research.

Since 2000, the Robotics and Automation Laboratory at Tsinghua University has developed humanoid robots, THBIP-I (Tsinghua biped robot-I) and THBIP-II.

THBIP-I, the first-generation prototype, is a human-sized prototype with a height of 174 cm, a weight of 130 Kg, and has 32 DOFs [12]. It has achieved stable static walking with a velocity of 4.2 m/min and a step length of 0.35 m. Also, it has

the ability to climb stairs and shadowbox. THBIP-I is different from other humanoid robots because of its special screw-nut-link mechanism at the ankle joint. This complex mechanism was designed to achieve a high torque during certain walking phases. However, the unfixed transmission ratio of this mechanism also leads to the diversification of the transfer function of the ankle joint<sup>[13]</sup>, which restricts the joint position tracking ability of the robot.

To resolve this problem, THBIP-II, an infant-size second-generation prototype with a modified actuation and transmission system, has been developed (see Fig.1) [14]. This prototype focused on the system design integration, motion planning and improvements of locomotion performance, which will be described in detail.

This paper introduces the prototype design, mechanical modeling, and motion planning including the gait planning method and global footstep planning, of THBIP-II humanoid. The following sections are organized as follows: Section II describes the prototype design; Section III describes the kinematics and dynamics modeling; Section IV describes the gait planning method; Section V presents the global footstep planning method; Section VI addresses walking experiments of the prototype.

## II. THE HUMANOID PROTOTYPE

### A. Conceptual Design

THBIP-II is an infant-size prototype which is 70 cm in height and 18 Kg in weight (see Fig.1(a)). The relative proportions of different parts are similar to human bodies [15].

The robot is equipped with 24 DOFs. There are 6 DOFs at each leg: two ankle DOFs (pitch and roll), one knee DOF (pitch), three hip DOFs (pitch, roll and yaw) (see Fig.1(b)). The leg DOFs make the robot adaptive to walking on the ground, turning in any direction and climbing up and down stairs [16]. The DOFs of the upper limbs and hands allow the robot to perform some manipulations such as grasping and moving objects.

### B. Hardware Realization

The actuators of the lower limbs were selected based on the simulation of several specific walking patterns in the sagittal and lateral plane. Contrary to the lower limbs, the design of the

upper body was focused on compact structure rather than power analysis.

Two miniature six-axis force/moment sensors are placed in the feet to measure the ground reaction force and utilized to compute the ZMP (Zero Moment Point) position during walking [2][16]. A strapped inertial navigation system is utilized in THBIP-II to measure real-time gestures. The inertial measurement units (IMU) are located on the upper limbs to measure rotational velocity relative to the inertial coordinate frame system and the acceleration relative to the body-fixed coordinate frame system by a gyroscope and accelerometers.

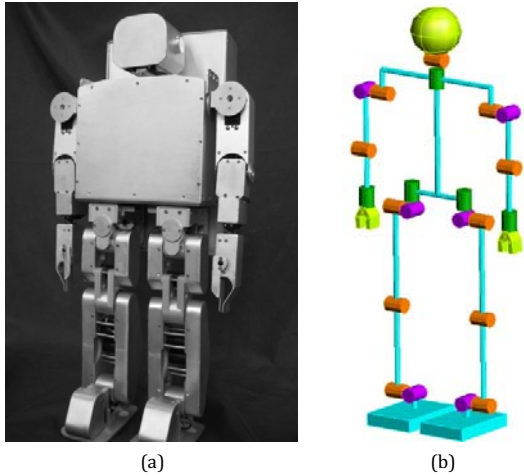


Fig. 1. THBIP-2 Prototype (a) and structure of THBIP-II (b)

A CAN bus-based distributed control system was designed (see Fig.2). The main PC performs the tasks of interface management, decision making, gait planning and status display. The motion controllers calculate the motor control signals according to the desired gait data from the main PC and position feedback data from the incremental encoders. The embedded DSP processors perform low-level computation of the sensing data. The gait data, joint status, and sensing data are transferred by the CAN bus. Joint status data are shared within motion controllers by first-in first-out (FIFO) memories.

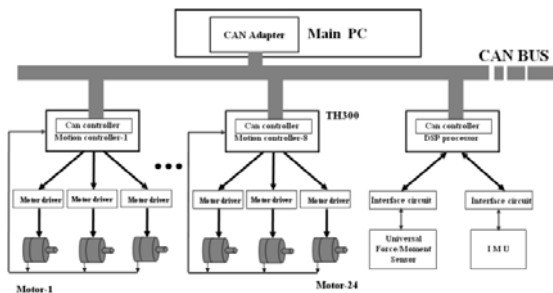


Fig.2 CAN Bus Based Distributed Control System of THBIP-II

### III. MECHANICAL MODELING ANALYSIS

#### A. Structure and Coordinate Frame Definition

Traditional link models describe the mechanical systems of humanoid robots in two separate planes, the sagittal and lateral

plane. However, when there is more than one DOF at the hip and ankle joints, this characteristic will cause singular solutions when decoupling the Euler angles into the desired control inputs. Consequently, a complete 3-Dimension 15-rigid-body model of THBIP-II was built (see Fig.1(b)). Each arm is considered as only one rigid body in this model, because our current research is focused on walking using the lower limbs only.

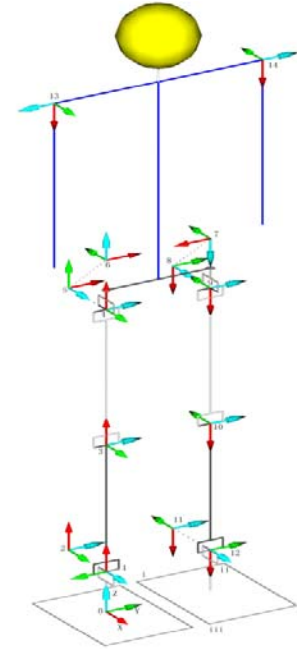


Fig. 3 The coordinate frames definition

Fifteen coordinate frames, numbered from 0 to 14, are defined, each of which is fixed to a corresponding rigid-body of the robot with the same number (see Fig.3). In the coordination definitions, each coordinate frame, namely each rigid body, can only rotate around its Z-axis relative to the pre-adjacent body-coordinate frame. The motion of the robot is realized by the fixed-axis rotation, which is the relative motion between coordinate frame  $i$  and coordinate frame  $i+1$ . The coordinate frame 0 is the world coordinate frame and is fixed to the right foot which keeps relatively static with the ground. With the above 15-rigid-body model, the kinematics description can be obtained. Also, the dynamic description of the robot can be obtained based on the Newton-Euler equations.

#### B. Kinematic Description

According to the above coordination definition, the relative motions between the 15 rigid bodies of the robot can be expressed by the direction cosine matrixes. The relative motions between coordinate frame 0 and 1, and between coordinate frame 1 and 2 are given as examples.

$$G_{0-1} = \begin{bmatrix} 0 & 0 & 1 \\ -\sin\theta_1 & -\cos\theta_1 & 0 \\ \cos\theta_1 & -\sin\theta_1 & 0 \end{bmatrix} \quad (1)$$

$$G_{1\_2} = \begin{bmatrix} \cos\theta_2 & -\sin\theta_2 & 0 \\ 0 & 0 & -1 \\ \sin\theta_2 & \cos\theta_2 & 0 \end{bmatrix} \quad (2)$$

The direction cosine matrixes have attributes as:

$$G_{j\_k} = \prod_{i=j}^{k-1} G_{i\_i+1} \quad (3)$$

$$G_{j\_k} = G_{k\_j}^T = G_{k\_j}^{-1} \quad (4)$$

where,  $\theta_i$  is the angle that the coordinate frame  $i$  has rotated relatively to coordinate frame  $i-1$ , and  $G_{j\_k}$  is the direction cosine matrix which represents the orientation of the coordinates frame  $k$  in coordinate frame  $j$ .

The position vector of the centroid of rigid body  $i$  in coordinate frame  $0$ ,  $r_{0\_i}$ , is computed as:

$$r_{0\_i} = l_{0\_1} + \sum_{k=1}^{i-1} G_{0\_k} \times l_{k\_k+1} + G_{0\_i} \times r_{i\_i} \quad (5)$$

where,  $l_{i\_j}$  is the position vector of origin of coordinate frame  $j$  in coordinate frame  $i$ , and  $r_{i\_j}$  is the position vector of the centroid of rigid body  $j$  in coordinate frame  $i$ .

The inertia tensor matrix of rigid-body  $i$  relatively to the origin of the world coordinate frame,  $J_{0\_i}$ , is computed as:

$$J_{0\_i} = G_{0\_i} \times J_{i\_i} \times G_{0\_i}^T \quad (6)$$

where,  $J_{i\_i}$  is the inertia tensor matrix of rigid-body  $i$  relative to the origin of coordinate frame  $i$ , which is a constant according to the actual prototype mechanism.

The angular velocity and angular acceleration is computed as:

$$\omega_{s\_t} = \sum_{s=i+1}^j G_{0\_s} Z \dot{\theta}_i \quad (7)$$

$$\alpha_{s\_t} = \sum_{i=s+1}^t G_{0\_i} Z \ddot{\theta}_i \quad (8)$$

where,  $\omega_{s\_t}$  and  $\alpha_{s\_t}$  are the angular velocity and angular acceleration of rigid-body  $t$  in coordinate frame  $s$  separately, and  $\dot{\theta}_i$  and  $\ddot{\theta}_i$  are the angular velocity and angular acceleration of rigid-body  $i$  in coordinate frame  $i$  separately.

The centroid velocity of each rigid body is computed as:

$$v_{i\_i+1} = \omega_{i\_i+1} \times (G_{i\_i+1} r_{i+1\_i+1}) \quad (9)$$

$$v_{i\_i+1+k} = \omega_{i\_i+1} \times G_{i\_i+1} r_{i+1\_i+1+k} + G_{i\_i+1} v_{i+1\_i+1+k} \quad (10)$$

where,

$$r_{s\_t} = l_{s\_s+1} + \sum_{k=s+1}^{t-1} G_{0\_k} \times l_{k\_k+1} + G_{s\_t} \times r_{t\_t} \quad (11)$$

and  $v_{i\_j}$  is the centroid velocity of rigid-body  $j$  in coordinate frame  $i$ .

The centroid acceleration of each rigid body is computed as:

$$a_{i\_i+1} = \alpha_{i\_i+1} \times (G_{i\_i+1} r_{i+1}^{i+1}) + \omega_{i\_i+1} \times (\omega_{i\_i+1} \times (G_{i\_i+1} r_{i+1}^{i+1})) \quad (12)$$

$$a_{i\_i+1+k} = \alpha_{i\_i+1} \times (G_{i\_i+1} r_{i+1\_i+1+k}) + \omega_{i\_i+1} \times (\omega_{i\_i+1} \times (G_{i\_i+1} r_{i+1\_i+1+k})) + 2\omega_{i\_i+1} \times (G_{i\_i+1} v_{i+1\_i+1+k}) + G_{i\_i+1} a_{i+1\_i+1+k} \quad (13)$$

When  $i=0$ , the above variables are absolute values in the world coordinate frame.

### C. Dynamic Description

Based on the above kinematics description of the mechanical model, forces and moments acted on each rigid body can be computed by Newton-Euler equations. Consequently, the driving torques and the constraint forces can be obtained.

The rigid-body at the end of the kinetic chain only comes under the force and moment exerted by one internal rigid-body of the kinetic chain.

$$F_0^{i \rightarrow i+1} = -m_{i+1} g_0 - F_0^{i+2 \rightarrow i+1} + m_{i+1} a_{0\_i} \quad (14)$$

$$M_0^{i \rightarrow i+1} = -F_0^{i \rightarrow i+1} \times (G_{0\_i+1} r_{i+1\_i+1}) - F_0^{i+2 \rightarrow i+1} \times (G_{0\_i+1} (r_{i+1\_i+1} - l_{i+1\_i+2})) - M_0^{i+2 \rightarrow i+1} + J_{0\_i} \alpha_{0\_i} + \omega_{0\_i} \times (J_{0\_i} \omega_{0\_i}) \quad (15)$$

where,  $m_i$  is the mass of rigid body  $i$ ,  $g_0 = [0 \ 0 \ -9.8]^T$  is the gravity vector, and  $F_i^{j \rightarrow k}$  and  $M_i^{j \rightarrow k}$  are the force and torque acting on rigid body  $k$  by rigid-body  $j$  in coordinate frame  $i$  respectively.

The force and torque expressions have attributes:

$$F_0^{i \rightarrow i+1} = -F_0^{i+1 \rightarrow i} \quad (16)$$

$$M_0^{i \rightarrow i+1} = -M_0^{i+1 \rightarrow i} \quad (17)$$

Also, the reaction force and moment from the ground can be computed as:

$$F_0^{ground \rightarrow 0} = -m_0 g_0 - F_0^{1 \rightarrow 0} \quad (18)$$

$$M_0^{ground \rightarrow 0} = -F_0^{ground \rightarrow 0} \times r_0^0 - F_0^{1 \rightarrow 0} \times (r_0^0 - l_{0\_1}) - M_0^{1 \rightarrow 0} \quad (19)$$

Detailed dynamics expressions in the single- and double-supporting phase can be deduced based on [14] - [19].

## IV. GAIT PLANNING

### A. Gait Planning Method

ZMP is the stability criterion of gait planning method for THBIP-II. The ZMP position computation can be seen in [18].

Unlike the gait planning algorithm for THBIP-I [19], the planned gait of THBIP-II is more similar to that of the human walking. During the walking of THBIP-I, the feet are always defined to be level with the ground (see Fig.4). According to a study on human walking [20], this walking mode is not feasible for fast walking. Furthermore, from the viewpoint of aesthetics, it is not desirable that the foot slope always be level.

In the gait planning algorithm for THBIP-II, the robot touches the ground first with the heel of the forward foot and then leaves the ground by the toe of the latter foot (see Fig.5). The planning in the sagittal plane is implemented based on the pre-definition of foot trajectory. It is processed as follows: **Step 1:** The trajectories of the feet, including the positions and angles of the feet are planned; **Step 2:** The trajectories of the

hips, which must ensure the robot posture to satisfy the ZMP criterion, is planned; **Step 3**: All other joint trajectories are computed according to the kinematic constraints. The planning in the lateral plane is done likewise and the three-order spline interpolation is utilized during the above trajectory generation.

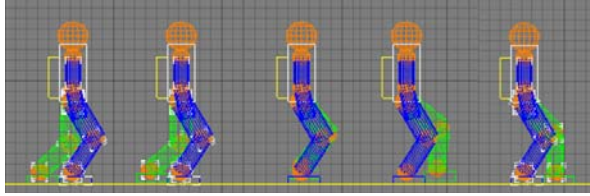


Fig.4 Walking Pattern with Soles to be Level

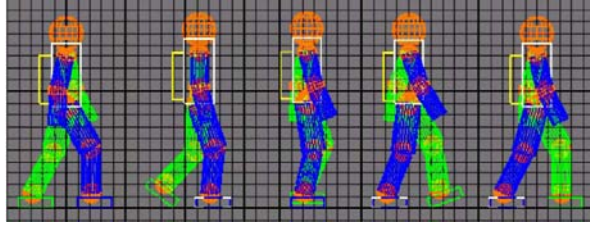


Fig.5 Walking Pattern with Nature Sole Orientation

### B. Planning Simulation

The planning simulation is processed with walking indexes listed in Tab.1. The interval of the double-supporting phase is 30%, which is similar to human locomotion [20]. A whole planning cycle includes a single-supporting phase and two double-supporting phases, 2.6 s as showed in Tab.1, in order to ensure the completeness of three-order spline interpolation and the smoothness of the phase switch.

Fig.6 is the stick figure of a walking cycle, in which the torso trajectory is similar to the sine curve, identical to our analysis of human body locomotion [21]. Fig.7 and Fig. 9(a) show the foot position and orientation during **step 1**. Fig.8 shows the hip position during **step 2**. Fig.9 (b) shows the angle of the supporting ankle in the lateral plane. Fig.10 shows the angle, rotational velocity and rotational acceleration of the ankle, knee and hip joints in the sagittal plane.

Tab.1 Gait Planning Indexes

Item	Value
Step length	0.16 m
Walking cycle	2 s
Single-supporting phase duration	1.4 s
Double-supporting phase duration	0.6 s
Planning duration	2.6 s

## V. GLOBAL FOOTSTEP PLANNING

### A. Footstep Planning Method

The realization of global navigation is based on the footstep planning method by Kuffner, et al (more details can be seen in [22]-[24]), which ignores the robot's kinematics and represents the robot by discrete footsteps.

The footstep planning method builds a search tree which is originated from the initial footstep and expanded according to a

pre-defined discrete set of potential footstep placements relative to the supporting foot, i.e., footstep transition model. The footstep nodes which lead to collision is pruned from the tree by collision checking based on the robot state and environment information. Using configured cost for each node, an optimal sequence of footstep placements can be computed. Finally pre-planned trajectory based on the above gait planning method is interpolated for gesture transitions between placements in the above footstep sequence.

### B. Footstep Transition Model

In footstep planning space, a supporting footprint  $\mathcal{F}$  is denoted as:

$$\mathcal{F} = (x, y, \theta, \zeta)^T \in \mathbb{R}^3 \times \mathbb{N}, \quad (20)$$

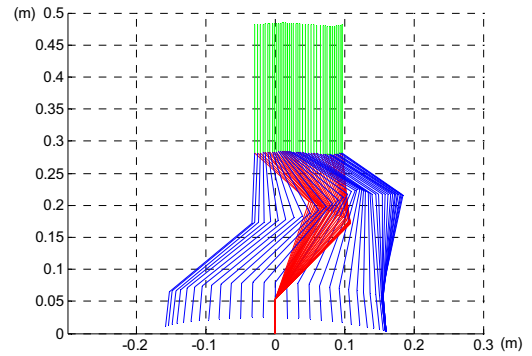


Fig.6 Stick figure of a walking cycle

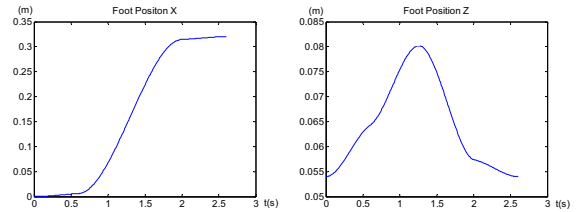


Fig.7 Foot position in the sagittal plane

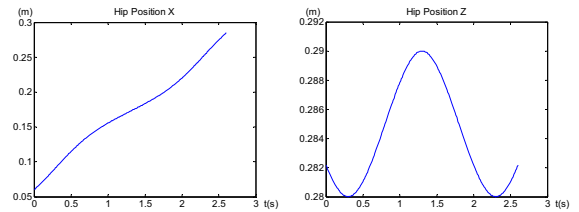


Fig.8 Hip position in the sagittal plane

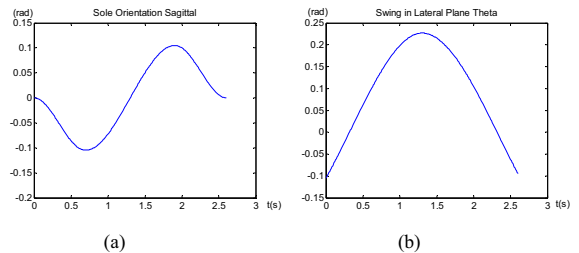


Fig.9 Foot orientation in the sagittal plane (a) and the angle of the supporting ankle in the lateral plane (b)

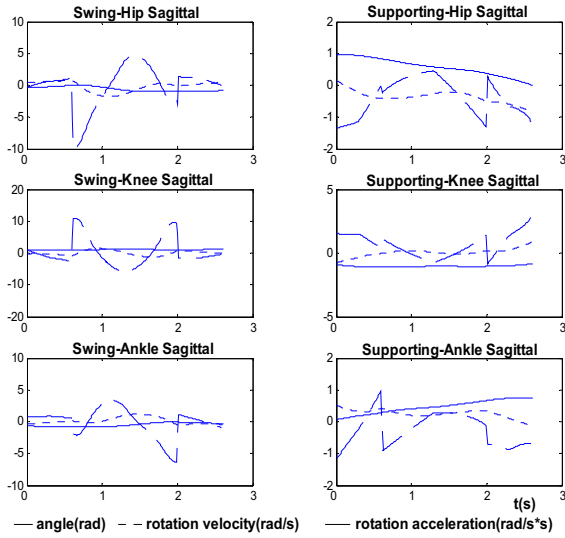


Fig.10 Kinematics data of ankle/knee/hip in the sagittal plane

where  $(x, y, \theta)$  is the footprint position and, and the discrete variable  $\zeta \in \{L, R\}$  stands for the supporting foot,  $L$  for the left foot and  $R$  for the right foot.

Similar to the operation space analysis of industrial robots, when the humanoid robot is supported by one foot, the reachable placements of the swing foot center will be limited in a specific area (see dotted moon-like area in Fig.11). The shape of the feasible area is affected by (1) physical parameters of the robot, e.g. geometrical length and mass distribution, (2) dynamical and kinematic parameters, e.g. the feasible rotational range and the actuation ability of each DOF, and (3) legged locomotion stability criterion, e.g., ZMP criterion [2].

The number of selected footstep placements determines the branching factor of the search tree, which exponentially affects the computational complexity of the search [22]. We configured a compound model, denoted as  $\mathcal{T}$ , with four sets of feasible footstep placements with 5 ( $\mathcal{T}_a$ ), 10 ( $\mathcal{T}_b$ ), 13 ( $\mathcal{T}_c$ ), and 25 ( $\mathcal{T}_d$ ) footprints separately (see Fig.3, the strip rectangles stand for the supporting footprints). Each set is the proper subset of the following sets.

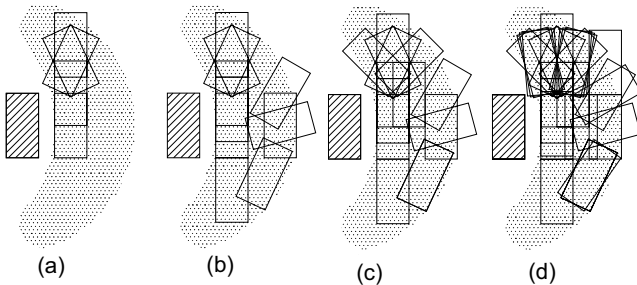


Fig.11 Configuration of potential footstep placements

The compound footstep transition model is configured based on the numerical simulation of planning in obstacle-clustered environments. The calling statistic of different footstep placements is similar to normal distribution, which means an

optimal sequence calls the footstep placements included in  $\mathcal{T}_a$  with a high probability, but the planning fails if only with  $\mathcal{T}_a$ . The dynamical calling of  $\mathcal{T}_a, \mathcal{T}_b, \mathcal{T}_c,$  and  $\mathcal{T}_d$  is according to a function is used to assess the expanded reachable area.

### C. Planning Simulation

The simulation was performed with a grid map of  $5m \times 5m$  with a resolution of  $0.01m$ . The planning was realized by A\* [25], in planning of Fig.12 and Fig.13, and Rapidly-exploring Randomized Trees (RRT) algorithm [26], specifically in areas with local minima or narrow passages, in planning of Fig.14 and Fig.15. Algorithms realization details can be seen in [24].

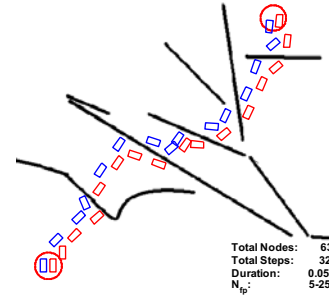


Fig.12 Footstep sequence in a low strip obstacles-clustered area

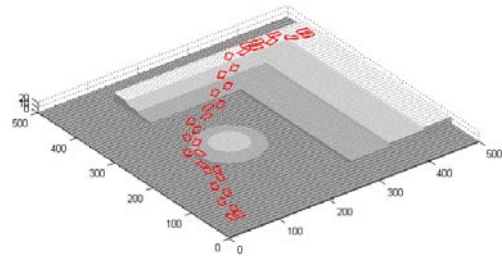


Fig.13 Footstep sequence in a platform with varying heights

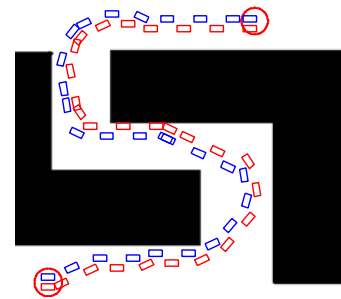


Fig.14 Footstep sequence in an area with narrow passage

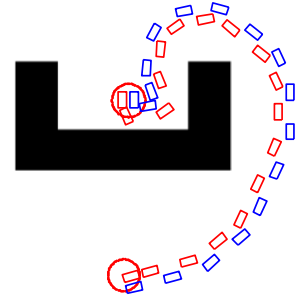


Fig.15 Footstep sequence in an area with local minima

## VI. EXPERIMENTS

The presented gait planning method has been verified in experiments. Stable walking with a step length of 0.16 m at a velocity of 2 s/step has been achieved. Fig.16 is a video snapshot of THBIP-II walking with the above parameters. Also, the same planning algorithm and control method was utilized in a robot soccer match. Fig.17 shows THBIP-II taking a penalty kick.

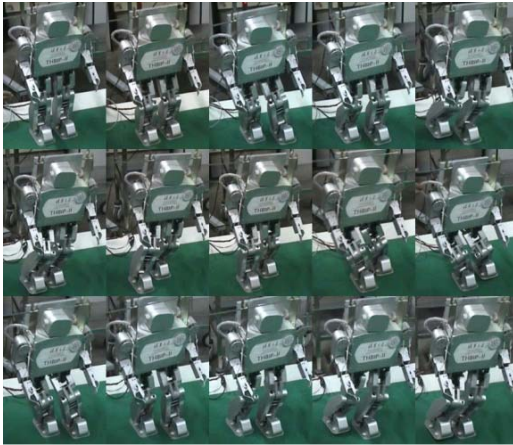


Fig.16 THBIP-II in walking

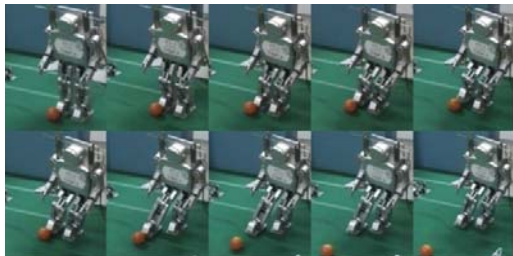


Fig.17 THBIP-II taking a penalty kick

## VII. CONCLUSION AND FUTURE WORK

The prototype realization, kinematics and dynamics modeling, gait planning method and global footstep planning methods implemented on humanoid robot THBIP-II were systematically addressed in this paper. THBIP-II is currently used as a platform for multi research focuses. Specifically, the online footstep planning with external vision system will be implemented on it.

## REFERENCES

- [1] I. Kato, "Development of Wabot-1," *Biomechanism 2*, The University of Tokyo Press, 1973, pp.173-214.
- [2] M. Vukobratovic, B. Borova and D. Surdilovic, "Zero-moment point-proper interpretation and new application", In *Proc. IEEE-RAS International Conference on Humanoid Robots*, pp.237~244, 2001.
- [3] T. McGeer, "Passive dynamic walking", *International Journal of Robotics Research*, pp.62-82,1990, 9(2)
- [4] B. Espiau, P. Sardain, "The biped robot BIP2000". In *Proc.Int. Conference on Advanced Robotics*, pp.971-976, 2000.

- [5] J. Pratt, "Virtual model control of a biped walking robot", *Doctoral Thesis*, Department of Electrical Engineering and Computer Science, Massachusetts Institute of Technology, Cambridge, Massachusetts, 1995.
- [6] C. L. Fu, "Section-map stability criterion and its Application for Dynamic Walking of Planar Biped Robots", *Doctoral Thesis*, Department of Precision Instruments and Mechanology, Tsinghua University, Beijing, 2007.
- [7] K. Hirai, M. Hirose, Y. Haikawa, et al, "The development of Honda humanoid robot". In *Proc. IEEE International Conference on Robotics and Automation*, 1998 May 16-20, Leuven, Belgium, 1998, pp.1321-1326.
- [8] T. Ishida, Y. Kuroki and J. Yamaguchi, "Mechanical system of a small biped entertainment robot", In *Proc. 2003 IEEE/RSJ International Conference on Intelligent Robot and Systems*, Las Vegas, Nevada, October 2003.
- [9] G. Wang, Q. Huang, J.H. Geng, et al. "Cooperation of dynamic patterns and sensory reflex for humanoid walking", In *Proc. IEEE International Conference on Robotics and Automation*, 2003, pp.2472-2477.
- [10] D. G. Caldwell, N. Tsagarakis, D. Badihi, et al, "Pneumatic muscle actuator technology: a lightweight power system for a humanoid robot", In *Proc. IEEE International Conference on Robotics and Automation*, pp.3035-3058, Leuven, Belgium, 1998.
- [11] S. Yashika, W. Ryujin, A. Chiaki, et al, "The intelligent ASIMO: system overview and integration". In *Proc. IEEE/RSJ International Conference on Intelligent Robots and Systems*, pp.2478-2483, 2002.
- [12] L. Liu, J. S. Wang, K. Chen, et al, "The research on the biped humanoid robot THBIP-I", *Robot*, Vol. 24, No.3, May 2002
- [13] J. D. Zhao, Z. Liu, C. L. Fu. "Self-regulating fuzzy control of a biped humanoid robot based on ZMP Error". In *Proc. 2006 Int'l Symposium on Artificial Life and Robotics*. Oita, Japan. pp.695-698, 2006.
- [14] Z.Y. Xia, L. Liu, J. Xiong and K. Chen, "Design aspects and development of humanoid robot THBIP-2", *Robotica*, Vol.26 (1), Jan.2008. pp.109-116.
- [15] V. Zatsiorsky and V. Seluyanov, "The mass and inertia characteristics of the main segments of the human body". *Biomechanics* 1983, 8, pp.1152.
- [16] R. Fred, J. Sias and Y. F. Zheng, "How many degrees-of-freedom does a biped need". In *Proc.1990 IEEE International Workshop on Intelligent Robots and System*.
- [17] S. Kajita, H. Hirukawa, K. Yokoi, *Humanoid robots*, Ohm-sha Ltd, 2005.
- [18] Q. Li, A. Tkanishi and I. Kato, "Development of ZMP measurement system for biped walking robot using universal force-moment sensors". *Journal of the Robotics Society of Japan*, Vol.10 (6), pp.828-833, 1992.
- [19] K. Xu, K. Chen, J. S. Wang, et al, "A new method of gait generation for a biped walking robot", In *Proc. 2th IEEE-RAS International Conference on Humanoid Robots*, Tokyo, Japan, Nov. pp.22-24 2001.
- [20] V. T. Inman, H. J. Ralston and F. Todd, *Human walking*. Baltimore, MD: Willams and Wilkins, 1981.
- [21] Z.Y. Xia, K. Chen, L. Liu, et al "Experimental analysis on human locomotion for natural gait planning of humanoid robots", *Robot*, Vol. 30(1), Jan. 2008. pp. 457-462
- [22] J.J. Kuffner, K. Nishiwaki, S. Kagami, et al, "Motion planning for humanoid robots", *Robotics Research*, Paolo Dario and Raja Chatila (Eds.), Springer Tracts in Advanced Robotics, vol. 15, pp.365-374, 2005
- [23] J. Chestnutt, J. J. Kuffner, K. Nishiwaki, et al, "Planning biped navigation strategies in complex environments" in *Proc. of IEEE Int. Conf. on Humanoid Robotics*, 2003.
- [24] Z. Y. Xia, K. Chen, "Modeling and algorithm realization of footstep planning for humanoid robots", *Robot*, 2008. ( in press)
- [25] N. Nilson, "Artificial Intelligence: A New Synthesis", Morgan Kaufmann, 1998.
- [26] S. M. LaValle, J. J. Kuffner. "Rapidly-exploring random trees: progress and prospects". In *Proc. Int. Workshop Alg. Found. Robot*, March 2000.